COMPUTER RESEARCH AND MODELING
2023 VOL. 15 NO. 1 P. 111–124
DOI: 10.20537/2076-7633-2023-15-1-111-124

КиМ

ANALYSIS AND MODELING OF COMPLEX LIVING SYSTEMS

UDC: 577.31, 577.38, 51-76

Bistability and damped oscillations in the homogeneous model of viral infection

A. A. Tokarev[1,2,3,a], N. O. Rodin[1,b], V. A. Volpert[1,4,c]

[1]Peoples' Friendship University of Russia (RUDN University),
6 Miklukho-Maklaya st., Moscow, 117198, Russia
[2]N. N. Semenov Federal Research Center for Chemical Physics RAS,
4/1 Kosygina st., 119991 Moscow, Russia
[3]Bukhara Engineering Technological Institute,
15 Murtazoyev st., Bukhara, 200100, Uzbekistan
[4]Institut Camille Jordan,
UMR 5208 CNRS, University Lyon 1, 69622 Villeurbanne, France

E-mail: [a] alexey.tokarev@mail.ru, [b] nikitarodin2013@yandex.ru, [c] volpert@math.univ-lyon1.fr

Received 25.05.2022, after completion — 06.10.2022.
Accepted for publication 13.12.2022.

The development of a viral infection in the organism is a complex process which depends on the competition race between virus replication in the host cells and the immune response. To study different regimes of infection progression, we analyze the general mathematical model of immune response to viral infection. The model consists of two ODEs for virus and immune cells non-dimensionalized concentrations. The proliferation rate of immune cells in the model is represented by a bell-shaped function of the virus concentration. This function increases for small virus concentrations describing the antigen-stimulated clonal expansion of immune cells, and decreases for sufficiently high virus concentrations describing down-regulation of immune cells proliferation by the infection. Depending on the virus virulence, strength of the immune response, and the initial viral load, the model predicts several scenarios: (a) infection can be completely eliminated, (b) it can remain at a low level while the concentration of immune cells is high; (c) immune cells can be essentially exhausted, or (d) completely exhausted, which is accompanied (c, d) by high virus concentration. The analysis of the model shows that virus concentration can oscillate as it gradually converges to its equilibrium value. We show that the considered model can be obtained by the reduction of a more general model with an additional equation for the total viral load provided that this equation is fast. In the case of slow kinetics of the total viral load, this more general model should be used.

Keywords: dynamics of viral infection, immune response, bistability, damped oscillations, mathematical modeling, qualitative analysis of ordinary differential equations

Citation: *Computer Research and Modeling*, 2023, vol. 15, no. 1, pp. 111–124.

This work was supported by the Russian Science Foundation project No. 22-21-00830, https://rscf.ru/en/project/22-21-00830/.

КОМПЬЮТЕРНЫЕ ИССЛЕДОВАНИЯ
И МОДЕЛИРОВАНИЕ 2023 Т. 15 № 1 С. 111–124
DOI: 10.20537/2076-7633-2023-15-1-111-124

Ки&М

АНАЛИЗ И МОДЕЛИРОВАНИЕ СЛОЖНЫХ ЖИВЫХ СИСТЕМ

УДК: 577.31, 577.38, 51-76

Бистабильность и затухающие колебания в гомогенной модели вирусной инфекции

А. А. Токарев[1,2,3,a], Н. О. Родин[1,b], В. А. Вольперт[1,4,c]

[1]Российский университет дружбы народов (РУДН),
Россия, 117198, Москва, ул. Миклухо-Маклая, д. 6
[2]Институт химической физики им. Н. Н. Семёнова РАН,
Россия, 119991, г. Москва, ул. Косыгина, д. 4
[3]Бухарский инженерно-технологический институт,
Узбекистан, 200100, Бухара, ул. Муртазаева, д. 15
[4]Институт Камиля Жордана,,
Франция, 69622, Вилеурбан, УМР 5208 НЦНИ, Университет Лион 1

E-mail: [a] alexey.tokarev@mail.ru, [b] nikitarodin2013@yandex.ru, [c] volpert@math.univ-lyon1.fr

Получено 25.05.2022, после доработки — 06.10.2022.
Принято к публикации 13.12.2022.

Развитие вирусной инфекции в организме представляет собой сложный процесс, зависящий от конкуренции между размножением вируса в клетках организма-хозяина и иммунным ответом. В данной работе для исследования различных режимов развития инфекции мы анализируем общую математическую модель иммунного ответа организма на вирусную инфекцию. Модель представляет собой систему из двух обыкновенных дифференциальных уравнений, описывающих изменение обезразмеренных концентраций вируса и иммунных клеток. Скорость пролиферации иммунных клеток представлена колоколообразной функцией концентрации вируса. Эта функция возрастает при малых концентрациях вируса, описывая антиген-стимулированную клональную экспансию иммунных клеток, и снижается при достаточно высоких концентрациях вируса, описывая подавление пролиферации иммунных клеток инфекцией. В зависимости от вирулентности вируса, силы иммунного ответа и начальной вирусной нагрузки, модель предсказывает несколько сценариев: (а) инфекция может быть полностью устранена, (б) она может оставаться на низком уровне при высокой концентрации иммунных клеток; (в) иммунная система может быть существенно истощена или (г) полностью истощена, что сопровождается (в, г) высокой концентрацией вируса. Анализ модели показывает, что концентрация вируса может колебаться по мере постепенного приближения к своему равновесному значению. Рассматриваемая модель может быть получена при редукции более общей модели — с дополнительным уравнением для общей вирусной нагрузки, в предположении, что общая вирусная нагрузка является быстрой переменной. В случае медленной кинетики общей вирусной нагрузки следует использовать указанную более общую модель.

Ключевые слова: динамика вирусной инфекции, иммунный ответ, бистабильность, затухающие колебания, математическое моделирование, качественный анализ систем обыкновенных дифференциальных уравнений

Работа выполнена при финансовой поддержке Российского научного фонда, проект № 22-21-00830, https://rscf.ru/project/22-21-00830.

1. Introduction

All organisms have an immune system that protects them against pathogens [Nicholson, 2016]. In this study, we particularly focus on immune protection against viruses. The general outcome of any viral infection is determined by the complex balance between the kinetics of virus reproduction inside the infected cells and spreading of the virus throughout the body, on the one hand, and the strength of the antiviral immune responses, on the other hand.

The immune system and the immune response are examples of very complex systems and processes that are being investigated by thousands of scientists worldwide. Let us briefly give a general idea of the complexity of this system. Two basic types, or phases, of immune response can be distinguished: innate and adaptive [Nicholson, 2016]. Innate immune response is fast and includes complement system activation, phagocytosis of pathogens (by macrophages, dendritic cells, and neutrophils), inflammation (monocyte activation and cytokine release by leukocytes), killing the pathogens and infected cells by natural killer cells, and activation of adaptive immune response by antigen-presenting cells. Adaptive immune response includes activation and clonal proliferation of T- and B-lymphocytes (CD4+ T-cells proliferate to helper T-lymphocytes, while CD8+ T-cells proliferate to cytotoxic T-lymphocytes), and production of antibodies by B-lymphocytes. Proliferated lymphocytes and produced antibodies are highly specific to the invaded antigen and act together to eliminate it.

Due to high complexity of the immune system, understanding its response to pathogens demands attraction of mathematical modeling methods [Bocharov et al., 2018b; Marchuk, 1991; Romanyukha, 2012]. In most cases, these models are based on ordinary differential equations (similarly to chemical kinetics models) describing concentrations of components — immune cells, cytokines, antibodies, etc. Frequently, a model contains time delay(s) because cell responses, as well as viral release from an infected cell, take some time after triggering.

As with any complex system, both “bottom-up” and “top-down” approaches are used in the contemporary mathematical modelling of the immune response. There exist quite complex mathematical models consisting of dozens of differential equations (“bottom-up” approach), as well as rather “simple” (“qualitative”, “phenomenological”, “conceptual”) mathematical models comprising only 2–3 differential equations (“top-down” approach) [Bocharov et al., 2018b; Marchuk, 1991; Romanyukha, 2012]. Top-down, conceptual models are useful for understanding the system properties in general. For example, using such “simple” models, existence of new behavior types of viral infections and immune response has recently been predicted and classified [Bocharov et al., 2017; Bocharov et al., 2018a]. However, the “simplicity” (only 2–3 equations) is confusing, because the high nonlinearity of equations, the presence of time delays, spatial non-uniformity and (usual for biology) problems of comparison with experimental data make these “simple” models very difficult to deal with. Thus, this “simple” models still contain lots of enigmas, and their behavior and properties should be studied in more detail.

In this work, we investigate the homogenous case of the recently proposed conceptual mathematical model of immune response to a viral infection capable of describing several outcomes of infection disease, from complete recovery to death [Bocharov et al., 2017; Bocharov et al., 2018a]. We systematically analyze the location of null-clines and consequent types of all the steady states in this system giving the above outcomes. We show that damped oscillations are possible during the transition to the steady state of incomplete recovery. We also show that this model can be obtained as a particular case of a more general model with an additional equation for the total viral load under the assumption that the total viral load is a fast variable, and in the case of slow kinetics of the total viral load, this more general model should be used.

2. Mathematical model

2.1. Model assumptions

We consider the homogeneous variant of the model proposed in [Bocharov et al., 2017; Bocharov et al., 2018a], based on the following assumptions (see Figure 1):

1. *Homogeneity*. Virus and immune cells are homogeneously distributed throughout the body.
2. *Time delays* are neglected.
3. *Replication of the virus*. Virus self-replicates by means of infected cells using their copying machinery. The model describes the total viral concentration (inside plus outside infected cells).
4. *Adaptive immunity*. Adaptive immune response consists of replication and cross-activation of many cell types (CD4+, CD8+, B-lymphocytes, etc.). In this model, only one type of immune cells is considered: cytotoxic T-lymphocytes (CTLs).
5. *Elimination of virus by the adaptive immunity*. CTLs kill the infected cells, thus eliminating viruses contained and replicating in them. Following Assumption 3, immune cells in this model are supposed to eliminate the virus directly.
6. *Proliferation of immune cells*. Clonal expansion of CTLs is induced by increasing virus concentration. The model supposes an increasing proliferation rate at low to intermediate virus concentrations.
7. *Inhibition of the immune response by virus concentration and by the total virus load*. The total viral load (virus presence in the organism for a prolonged period of time) is supposed to inhibit the proliferation of CTLs by shifting them to the anergy state and further to apoptosis [Bocharov, 1998]. The model presented in [Bocharov et al., 2017; Bocharov et al., 2018a] assumes this inhibition acting directly by high virus concentration. In this article, we study both approaches.
8. *Death of immune cells*. Immune cells die naturally, and viruses increase their death rate.

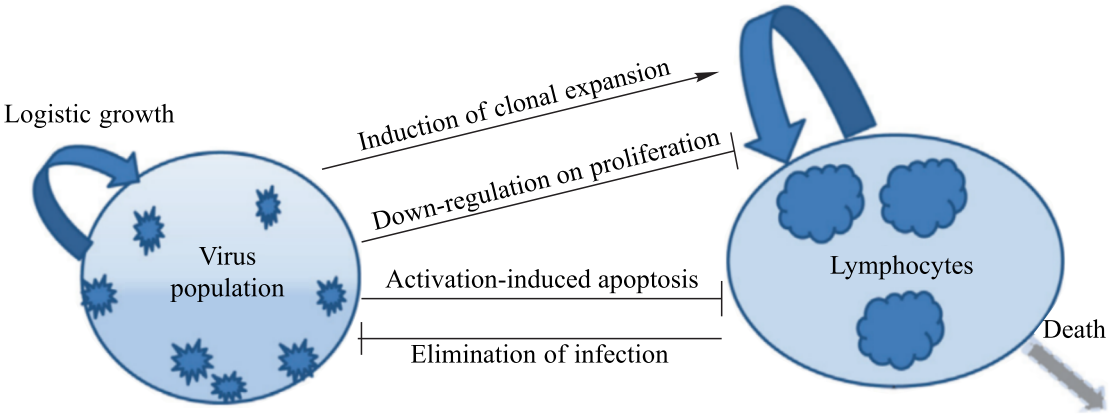

Figure 1. General scheme of the processes of viral infection and the antiviral immune response (from [Bocharov et al., 2017], with changes). According to this general scheme, viral infection, immune response, and interaction between them proceed through multiple positive and negative feedbacks (see the text above arrows). Thus, very complex properties should be expected even in the 2-variable model

2.2. Model equations

Following [Bocharov et al., 2017; Bocharov et al., 2018a], we consider the following system of equations:

$$\begin{cases} \dfrac{dv}{dt} = kv(1-v) - vc, \\ \dfrac{dc}{dt} = \varphi(v)c(1-c) - \psi(v)c. \end{cases} \tag{1}$$

Here, v is the virus concentration, c is the concentration of CTLs, k is the virus replication rate constant, $\psi(v)$ is the effective rate constant of CTL natural death and virus-dependent apoptosis, and $\varphi(v)$ is the effective rate constant of CTLs proliferation. The first term on the right-hand side of the first equation of the system (1) describes virus replication, and the last one describes virus elimination by immune cells. The first term on the right-hand side of the second equation describes the proliferation of immune cells, and the last term describes the death of immune cells.

CTLs replicate with the rate determined by the level of infection: low virus concentration stimulates the production of CTLs, and large one suppresses it. Therefore, it was suggested [Bocharov et al., 2017; Bocharov et al., 2018a] that the intensity of the immune response $\varphi(v)$ has a bell-shaped dependence on the concentration of the virus, that is, it increases at low and decreases at high infection levels.

A schematic phase portrait of this system is reproduced from [Bocharov et al., 2017; Bocharov et al., 2018a] in Fig. 2. The v-nullclines are given by the equations

$$v = 0 \quad \text{and} \quad c = k \cdot (1 - v) \tag{2}$$

and the c-nullclines are given by the equations

$$c = 0 \quad \text{and} \quad c = f(v) \tag{3}$$

where

$$f(v) = 1 - \frac{\psi(v)}{\varphi(v)}. \tag{4}$$

Below in this article we analyze this model in more detail.

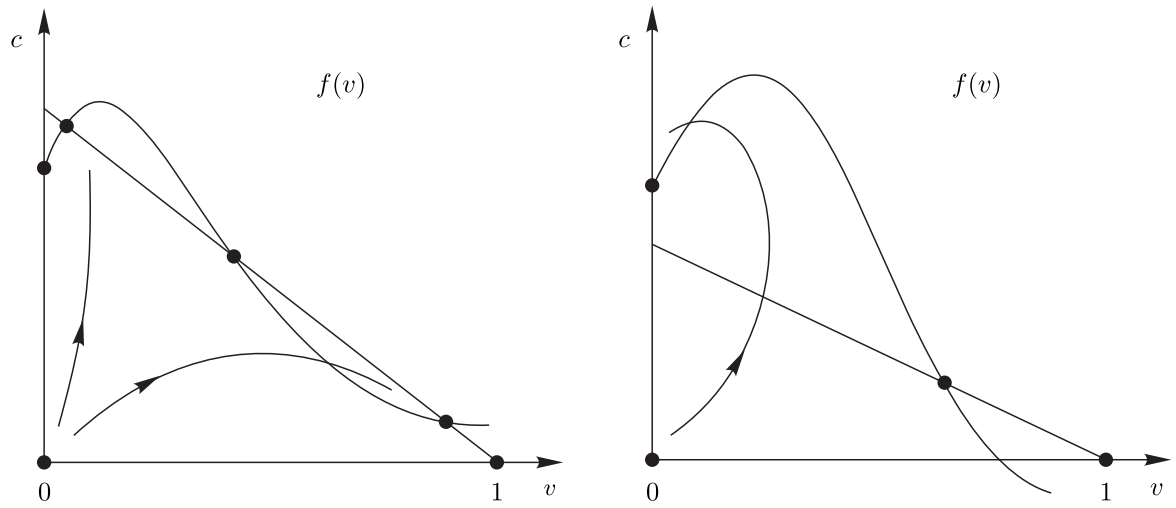

Figure 2. Schematic presentation of the phase plane of the initial model from [Bocharov et al., 2017]. There are 6 steady states in the left figure and 4 steady states in the right figure

2.3. Functions $\varphi(v)$ and $\psi(v)$

To reproduce the phase portraits shown in Fig. 2, *a* and *b*, we use two sets of kinetic functions $\varphi(v)$, $\psi(v)$. The first set is (see Fig. 3, *a*):

$$\begin{aligned} \varphi(v) &= \frac{p_0 + p_1 v}{1 - (e^{(-2.5v)} - 0.5e^{(-35v)})}, \\ \psi(v) &= p_0 + p_1 v \end{aligned} \tag{5}$$

which gives $f(v)$ as (see Fig. 3, *b*)

$$f(v) = e^{(-2.5v)} - 0.5e^{(-35v)}. \tag{6}$$

The second set is (see Fig. 4, *a*):

$$\begin{aligned} \varphi(v) &= (p_2 + p_3 v)e^{(-4v)}, \\ \psi(v) &= p_0 + p_1 v \end{aligned} \tag{7}$$

which gives $f(v)$ as (see Fig. 4, *b*)

$$f(v) = 1 - \frac{p_0 + p_1 v}{(p_2 + p_3 v)e^{(-4v)}}. \tag{8}$$

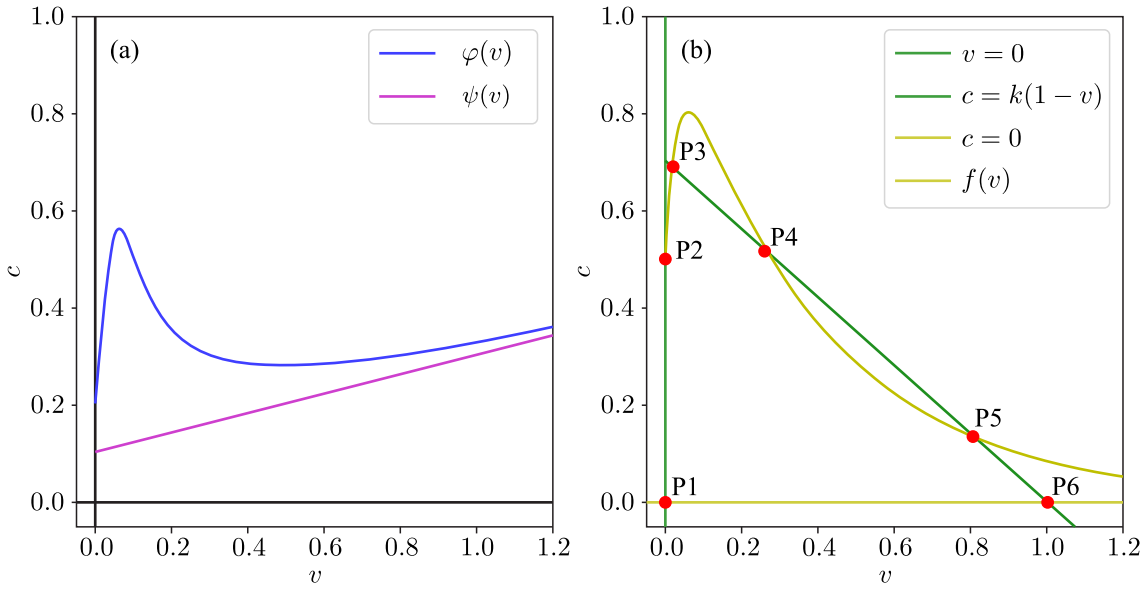

Figure 3. (a) functions $\varphi(v)$ and $\psi(v)$ from Eqs. (5). (b) null-clines and steady states of the system (1), (5); $f(v)$ corresponds to Eq. (6)

2.4. Particular kinetics of the total viral load

To obtain the extended version of the model [Bocharov et al., 2017; Bocharov et al., 2018a] which includes the total viral load, we replace v by w in the decreasing factor of the equation for $\varphi(v)$ in the second set of functions, and add the kinetic equation for $w(t)$ [Bocharov, 1998]. We get the

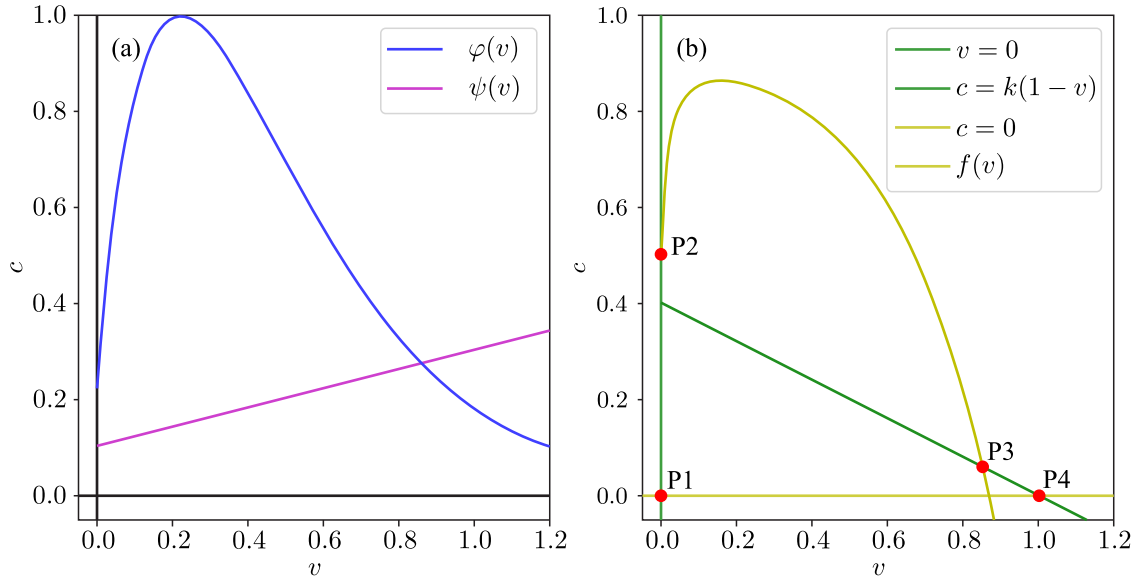

Figure 4. (a) functions $\varphi(v)$ and $\psi(v)$ from Eqs. (7). (b) null-clines and steady states of the system (1), (7); $f(v)$ corresponds to Eq. (8)

following model instead of Eqs. (1), (7):

$$\begin{cases} \dfrac{dv}{dt} = kv(1 - v) - vc, \\ \dfrac{dc}{dt} = \varphi(v,\, w)c(1 - c) - \psi(v)c, \\ \dfrac{dw}{dt} = \dfrac{bv - aw}{\varepsilon}, \\ \varphi(v,\, w) = (p_2 + p_3 v) \cdot e^{\left(-4\frac{a}{b}w\right)}, \\ \psi(v) = p_0 + p_1 v. \end{cases} \tag{9}$$

According to Tikhonov's theorem, these equations reduce to Eqs. (1) and (7) as $\varepsilon \to 0$.

2.5. Linear stability analysis

Steady states can be studied for their type and stability according to the first Lyapunov method. The Jacobi matrix for system (1) is

$$J = \begin{pmatrix} \frac{\partial V}{\partial v} & \frac{\partial V}{\partial c} \\ \frac{\partial C}{\partial v} & \frac{\partial C}{\partial c} \end{pmatrix}, \tag{10}$$

where $V = kv(1 - v) - vc$ and $C = \varphi(v)c(1 - c) - \psi(v)c$ are the right-hand sides of the differential equations defining the behavior of variables v and c. As a result, we get:

$$J = \begin{pmatrix} k(1 - 2v) - c & -v \\ \varphi'(v)c(1 - c) - \psi'(v)c & \varphi(v)(1 - 2c) - \psi(v) \end{pmatrix}. \tag{11}$$

The characteristic equation

$$|J - \lambda E| = 0 \tag{12}$$

solved for each of the steady states gives the pair of eigenvalues $\lambda_{1,2}$ which determine the type of this steady state.

2.6. Numerical methods

ODEs were numerically integrated in Python with the Solve_ivp function using the explicit Runge – Kutta method of order 5(4) (the error is controlled with the fourth-order accuracy, while the steps are taken with the fifth-order accuracy, local extrapolation is done) [Dormand, Prince, 1980]. For plotting, Python 3 Matplotlib library was used [Hunter et al., 2020]. For preliminary calculations, XPP/Auto was used [Ermentrout, 2002].

3. Results

3.1. Possible outcomes of viral infection depend on the null-clines' shape

To qualitatively reproduce the phase portraits presented in Fig. 2 from [Bocharov et al., 2017], we have chosen the formulas for functions $\varphi(v)$ and $\psi(v)$, determining $f(v)$ (Eq. (4)). To reproduce Fig. 2 (left), we have chosen Equations (5) (that is, the first set), and to reproduce Fig. 2 (right), we have chosen Equations (7) (that is, the second set). These functions are presented in Figs. 3, *a* and 4, *a*, and the corresponding null-clines of the system (1) are presented in Figs. 3, *b* and 4, *b*, respectively. There are 4 possible outcomes of illness:

1. Chronic latent infection, incomplete recovery (Fig. 3, *b*, steady state P3).
2. Severe infection with incomplete exhaustion of the immune system (Fig. 3, *b*, steady state P5).
3. Complete recovery (Fig. 4, *b*, steady state P2).
4. Lethal infection with complete exhaustion of the immune system (Fig. 4, *b*, steady state P4).

Pairwise, these outcomes can result in 4 cases of the phase portrait structure:

- Case 1 (outcomes 1 + 2),
- Case 2 (outcomes 3 + 4),
- Case 3 (outcomes 1 + 4),
- Case 4 (outcomes 3 + 2).

Below we investigate these four outcomes numerically and analytically.

3.2. Actual outcome of viral infection depends on the initial viral load

We numerically studied the domains (basins) of attraction of all the stable steady states in four cases outlined above: Case 1 (outcomes 1 + 2) — in Figure 5, *b*, Case 2 (outcomes 3 + 4) — in Figures 6, *a* and 6, *d*, Case 3 (outcomes 1+4) — in Figures 6, *b* and 6, *c*, and Case 4 (outcomes 3 + 2) — in Figure 5, *a*. In all figures, the trajectories are colored black, stable points are colored red, and the saddles are colored purple. We assumed that the initial condition of the system is some point (v_0, c_0) located close to the origin (the abscissa indicates the initial viral load, and the ordinate indicates the innate immune response), because the real initial viral load is some sporadic value, and the innate immune response helping to switch on the adaptive one is not considered explicitly in the model. In most calculations, we took values for v_0 and c_0 equally distributed in the section [0.01; 0.15] with a constant step, so the initial conditions were equally distributed in the square from (0.01, 0.01) to (0.15, 0.15). Sometimes we added one or two trajectories to make the figures clearer.

Figure 5, *a* and *b* shows that the behavior of phase trajectories depends on the value of the parameter k and on the initial conditions. In Fig. 5, *a* (k = 0.6), 4 out of 11 trajectories tend to the

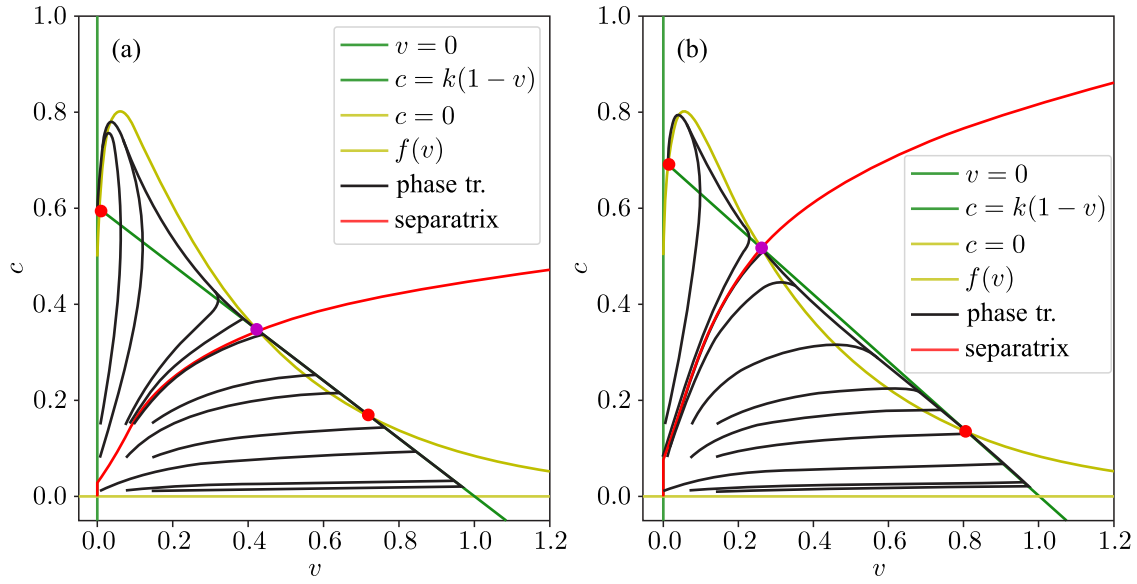

Figure 5. Phase planes (Eqs. (1), (5)) for different values of the parameter k = 0.6 (a) and k = 0.7 (b) and initial conditions located close to the origin. With increasing k, the saddle (purple) and its separatrix (red) move top-left, and more phase trajectories (black) tend to the bottom-right singular point (red). Other parameters are p_0 = 0.2 and p_1 = 0.1

top-left stationary point. This point corresponds to almost complete recovery, more precisely, to the chronic infection (a certain amount of the virus will remain in the organism). Initial conditions of these trajectories are located above the separatrix. The remaining 7 trajectories tend to the bottom-right stable point, and in this case there is substantial depletion of the immune system. In Fig. 5, *b*, the virus replication coefficient is increased to k = 0.7, and starting from the same initial data only 2 phase trajectories tend to the top-left stable steady state, while all other trajectories tend to the bottom-right one.

Figure 6, *a*–*d* shows that the behavior of the phase trajectories depends on the values of parameters k and p_3, as well as on the initial conditions. In Fig. 6, *a* (k = 0.4 and p_3 = 5), 8 out of 10 trajectories tend to the top-left steady state. This means that under such initial conditions (values of v_0 and c_0), the course of the disease will end in a complete recovery. Only two curves tend to the bottom-right steady state corresponding to the complete exhaustion of the immune system. In Fig. 6, *b*, the virus replication coefficient is increased to k = 0.8, and p_3 is the same as in Fig. 6, *a*. There, only 4 trajectories tend to the top-left steady state (which now corresponds to the chronic disease, since $v > 0$), and the remaining 6 trajectories tend to the bottom-right steady state (complete exhaustion of the immune system and death). In Fig. 6, *c*, *d*, the immune response is increased by setting p_3 = 10, and k = 0.8 and 0.4, respectively. In both cases, the saddle is shifted lower compared with Figs. 6, *a*, *b*, thus the majority of trajectories tend to the top-left steady states.

Figures 5 and 6 shows, that the particular outcome of the disease depends on the location of the initial conditions relative to the separatrix (red curve). The initial conditions located above the separatrix lead to top-left steady states (outcomes 1 and 3), while the initial conditions located below the separatrix lead to bottom-right steady states (outcomes 2 and 4).

3.3. Linear stability analysis predicts damped oscillations

Tables 1 and 2 contain eigenvalues for all the steady states of the system (1) found using the 1st Lyapunov method (Eqs. (10)–(12)). Table 1 contains eigenvalues for the first set of functions $\varphi(v)$, $\psi(v)$ (Eqs. (5)), steady states P_1–P_6 in Fig. 3, *b*: the point P_1 has coordinates (0; 0), the point P_2

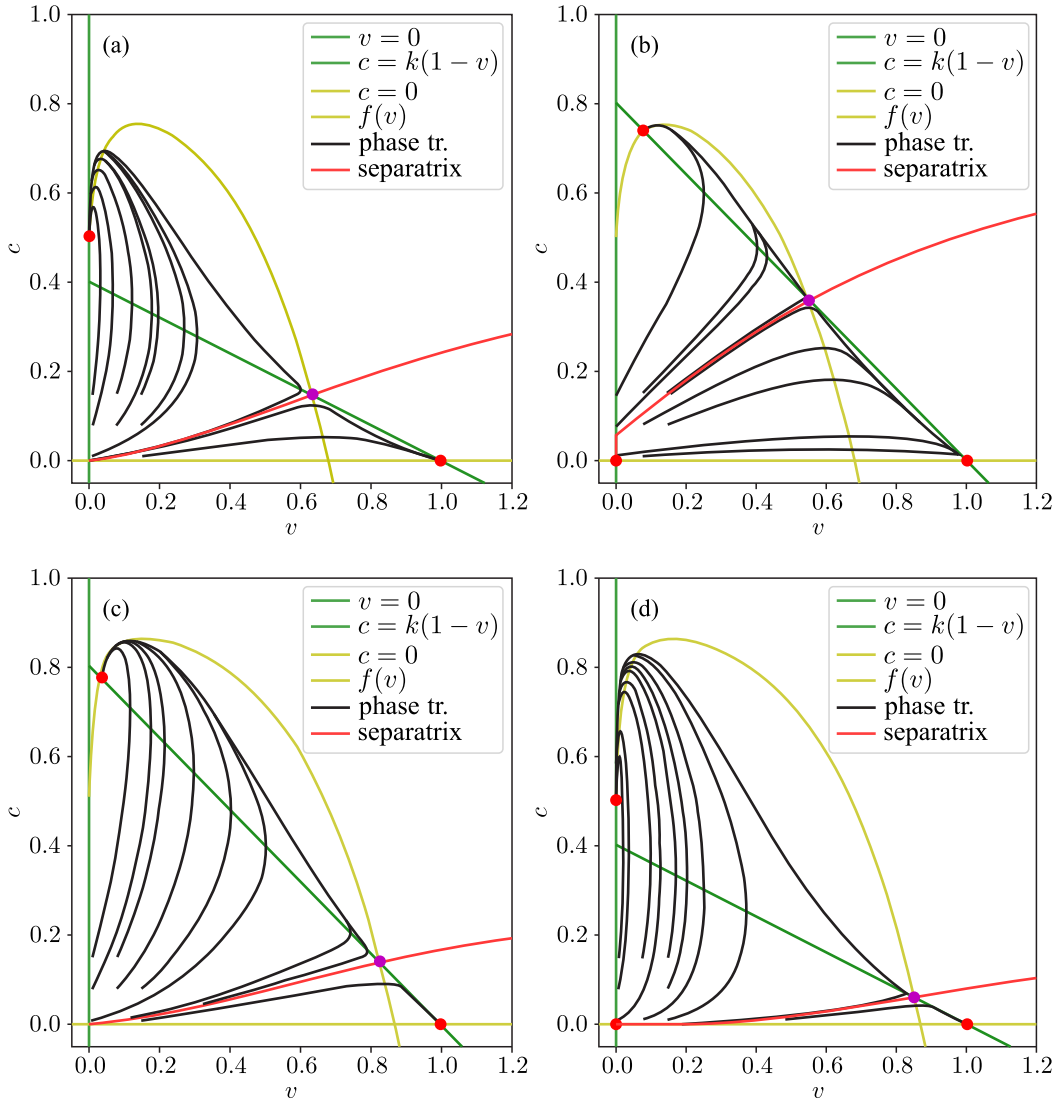

Figure 6. Phase planes (Eqs. (1), (7)) for different values of the parameters: (a) $k = 0.4$, $p_3 = 5$; (b) $k = 0.8$, $p_3 = 5$; (c) $k = 0.8$, $p_3 = 10$; and (d) $k = 0.4$, $p_3 = 10$. With increasing p_3, the immune response becomes stronger, and more phase trajectories (black lines) tend to the upper-left steady state (red point). Other parameters are: $p_0 = 0.2$, $p_1 = 0.1$, and $p_2 = 0.2$

has coordinates (0; $f(0)$), P_3 — (v_3; c_3), P_4 — (v_4; c_4), P_5 — (v_5; c_5), and P_6 — (1; 0); here, $0 < v_i < 1$; $0 < c_i < 1$ ($i = 3, \ldots, 5$; $i \leqslant 5$). Table 2 contains eigenvalues for the second set of functions $\varphi(v)$, $\psi(v)$ (Eqs. (7)), steady states P_1–P_4 in Fig. 4, *b*: the point P_1 has coordinates (0; 0), P_2 — coordinates (0; $f(0)$), P_3 — (v_3; c_3), P_4 — (1; 0). All eigenvalues are real except for those for point P_3 (corresponding to the 1^{st} outcome of the illness). Depending on parameters, eigenvalues for P_3 can be real negative or complex with negative real part indicating that this point can be either a stable node or a stable focus. In the latter case, this leads to damped oscillations of virus and immune cells concentrations as the system gradually converges to its equilibrium state.

3.4. Explicit consideration of the total viral load kinetics

Above, we have analyzed the system of two differential equations (Eqs. (1)). In this model, inhibition of the proliferation of immune cells by the increasing viral load is modeled by the declining

Table 1. Steady states of the system (1) with the first set of functions $\varphi(v)$, $\psi(v)$ (Eqs. (5)). Both cases, $k < f(0)$ and $k > f(0)$, are considered

Steady state	Coordinates	Eigenvalues		Type
		Formula	Value	
Case $k < f(0)$				
P_1	(0; 0)	$\lambda_1 = k$ $\lambda_2 = \varphi(0) - \psi(0)$	$0 < \lambda_1 < +\infty$ $\lambda_2 = 0.1$	Unstable node
P_2 $k < f(0)$	(0; $f(0)$)	$\lambda_3 = k - f(0)$ $\lambda_4 = \varphi(0)(1 - 2f(0)) - \psi(0)$	$\lambda_3 < 0$ $\lambda_4 = -0.02$	Stable node
P_3	(v_3; c_3)	$\lambda_7 = -k$ $\lambda_8 = \varphi(1) - \psi(1)$	$\lambda_5 < 0$ $\lambda_6 \approx 0.03$	Saddle
Case $k > f(0)$				
P_2 $k > f(0)$	(0; $f(0)$)	$\lambda_3 = k - f(0)$ $\lambda_4 = \varphi(0)(1 - 2f(0)) - \psi(0)$	$\lambda_3 > 0$ $\lambda_4 = -0.02$	Saddle
P_3 $f(0) < k < 0.53$	(v_3; c_3)	$\lambda_5 = \frac{a_3+b_3+\sqrt{(a_3-b_3)^2-4p_3}}{2}$ $\lambda_6 = \frac{a_3+b_3-\sqrt{(a_3-b_3)^2-4p_3}}{2}$	$\lambda_5 < 0$ $\lambda_6 < 0$	Stable node
P_3 $0.53 \leqslant k \leqslant 0.814$	(v_3; c_3)	$a_j = k(1 - 2v_j) - c_j$, $b_j = \varphi(v_j)(1 - 2c_j) - \psi(v_j)$, $p_j = v_j\varphi'(v_j)c_j(1 - c_j) - \psi'(v_j)c_j$, $3 \leqslant j \leqslant 5$, $j \in N$	$\lambda_5 = \alpha + \beta i$ $\lambda_6 = \alpha + \beta i$ ($\alpha < 0$)	Stable focus
P_3 $k \geqslant 0.815$	(v_3; c_3)		$\lambda_5 < 0$ $\lambda_6 < 0$	Stable node
P_4	(v_4; c_4)	$\lambda_7 = \frac{a_4+b_4+\sqrt{(a_4-b_4)^2-4p_4}}{2}$ $\lambda_8 = \frac{a_4+b_4-\sqrt{(a_4-b_4)^2-4p_4}}{2}$	$\lambda_7 > 0$ $\lambda_8 < 0$	Saddle
P_5	(v_5; c_5)	$\lambda_9 = \frac{a_5+b_5+\sqrt{(a_5-b_5)^2-4p_5}}{2}$ $\lambda_{10} = \frac{a_5+b_5-\sqrt{(a_5-b_5)^2-4p_5}}{2}$	$\lambda_9 < 0$ $\lambda_{10} < 0$	Stable node
P_6	(1; 0)	$\lambda_{11} = -k$ $\lambda_{12} = \varphi(1) - \psi(1)$	$\lambda_{11} < 0$ $\lambda_{12} \approx 0.03$	Saddle

part of the bell-shaped dependence $\varphi(v)$. Actually, this inhibition is determined by the total (i. e., accumulated) viral load [Bocharov, 1998]. In Eqs. (1), the total viral load w is indicated by the current virus concentration of v, i. e., w is considered implicitly — as a fast variable tracking v. In order to test this approach numerically, we have explicitly included the total viral load w into the model (Eqs. (9)).

For $0 < \varepsilon < 1$ (Fig. 7, *b–d*), the phase portraits are similar to the case $\varepsilon = 0$ (Fig. 7, *a*). However, for $\varepsilon \geqslant 1$ all trajectories tend to the upper-left steady state, and the domain of attraction of the bottom-right stable steady state is greatly reduced despite the fact that the bistability remains (Fig. 7, *e*, *f*). This indicates that transition from Eqs. (9) to Eqs. (1), (7) by means of Tikhonov's theorem is valid only if the kinetics of the total viral load is fast ($\varepsilon < 1$). In the case of slow kinetics of the total viral load ($\varepsilon \gtrsim 1$), the more detailed model (Eqs. (9)) should be used.

4. Discussion

Mechanisms of immune response to viral infection are insufficiently understood to date due to the high complexity of the immune system. This is true both for detailed mechanisms (on the molecular level), and for general ones (on the system's level). This situation strongly stimulates mathematical modelling in this field [Bocharov et al., 2018b; Marchuk, 1991; Romanyukha, 2012]. In this work, we

Table 2. Steady states of the system (1) with the second set of functions $\varphi(v)$, $\psi(v)$ (Eqs. (7)). Both cases, $k < f(0)$ and $k > f(0)$, are considered

Steady state	Coordinates	Eigenvalues		Type
		Formula	Value	
Case $k < f(0)$				
P_1	$(0; 0)$	$\lambda_1 = k$ $\lambda_2 = \varphi(0) - \psi(0)$	$0 < \lambda_1 < +\infty$ $\lambda_2 = 0.1$	Unstable node
P_2	$(0; f(0))$ $k < f(0)$	$\lambda_3 = k - f(0)$ $\lambda_4 = \varphi(0)(1 - 2f(0)) - \psi(0)$	$\lambda_3 < 0$ $\lambda_4 = -0.02$	Stable node
P_3	$(v_3; c_3)$	$\lambda_5 = \frac{a_3+b_3+\sqrt{(a_3-b_3)^2-4p_3}}{2}$ $\lambda_6 = \frac{a_3+b_3-\sqrt{(a_3-b_3)^2-4p_3}}{2}$	$\lambda_5 > 0$ $\lambda_6 < 0$	Saddle
P_4	$(1; 0)$	$\lambda_7 = -k$ $\lambda_8 = \varphi(1) - \psi(1)$	$\lambda_7 < 0$ $\lambda_8 \approx -0.11$	Stable node
Case $k > f(0)$				
P_2	$(0; f(0))$ $k > f(0)$	$\lambda_3 = k - f(0)$ $\lambda_4 = \varphi(0)(1 - 2f(0)) - \psi(0)$	$\lambda_3 > 0$ $\lambda_4 = -0.2$	Saddle
P_3	$(v_3; c_3)$ $f(0) < k \leqslant 0.53$	$\lambda_5 = \frac{a_3+b_3+\sqrt{(a_3-b_3)^2-4p_3}}{2}$ $\lambda_6 = \frac{a_3+b_3-\sqrt{(a_3-b_3)^2-4p_3}}{2}$	$\lambda_5 < 0$ $\lambda_6 < 0$	Stable node
P_3	$(v_3; c_3)$ $0.531 \leqslant k \leqslant 0.83$	$a_j = k(1 - 2v_j) - c_j$, $b_j = \varphi(v_j)(1 - 2c_j) - \psi(v_j)$, $p_j = v_j\varphi'(v_j)c_j(1 - c_j) - \psi'(v_j)c_j$, $3 \leqslant j \leqslant 4$, $j \in N$	$\lambda_5 = \alpha + \beta i$, $\lambda_6 = \alpha + \beta i$, $\alpha < 0$	Stable focus
P_3	$(v_3; c_3)$ $k \geqslant 0.831$		$\lambda_5 < 0$ $\lambda_6 < 0$	Stable node
P_4	$(v_4; c_4)$	$\lambda_7 = \frac{a_4+b_4+\sqrt{(a_4-b_4)^2-4p_4}}{2}$ $\lambda_8 = \frac{a_4+b_4-\sqrt{(a_4-b_4)^2-4p_4}}{2}$	$\lambda_7 > 0$ $\lambda_8 < 0$	Saddle
P_5	$(1; 0)$	$\lambda_9 = -k$ $\lambda_{10} = \varphi(1) - \psi(1)$	$\lambda_9 < 0$ $\lambda_{10} \approx -0.11$	Stable node

systematically study the qualitative properties of the previously developed general, phenomenological, model of the immune response to a viral infection consisting only of two ODEs [Bocharov et al., 2017; Bocharov et al., 2018a]. Despite its low dimension, this model is capable of describing four different outcomes of the infection disease: complete recovery, incomplete recovery (chronic latent infection), severe infection with incomplete exhaustion of the immune system, and lethal infection with complete exhaustion of the immune system. Thus, every type of behavior in this model has its physiological (medical) interpretation.

Firstly, we gave a systematic description of all the steady states and their basins of attraction depending on the parameter values in the model. We found the existence of oscillatory regime when approaching the steady state of incomplete recovery.

Secondly, we investigated the progression of the disease depending on the initial conditions (that is, the initial viral load and the level of the innate immune response), and showed that the outcome of the disease depends on the location of initial conditions with respect to the separatrix of the saddle point. Thus, the ultimate fate of infection can be very sensitive to the initial conditions in the case when they are close to a separatrix. This is important for prognosis of disease progression and for developing the measures to control it on both individual and population levels, such as wearing masks [Banerjee, Tokarev, Volpert, 2020].

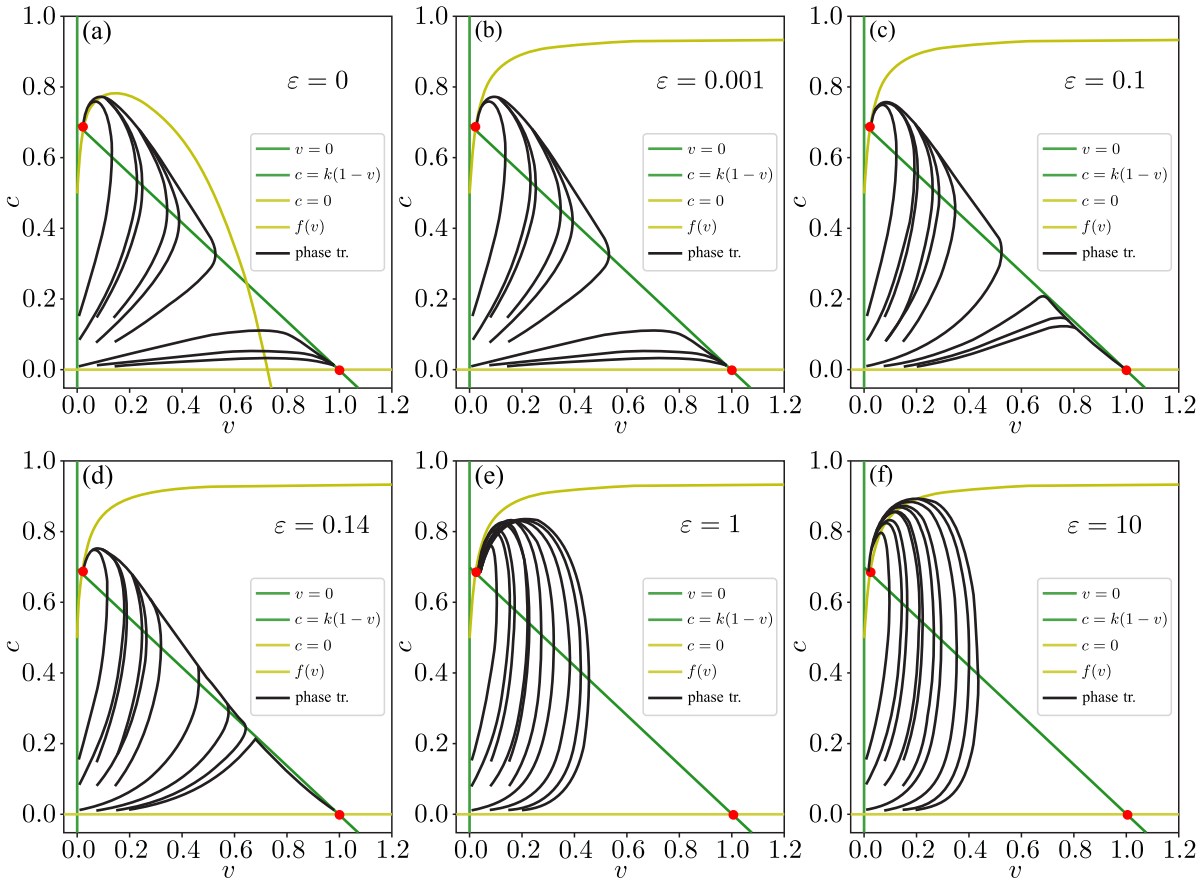

Figure 7. The behavior of projections of the phase trajectories for different values of ε: $\varepsilon = 0$ ((a), Eqs. (1)) and $\varepsilon > 0$ ((b)–(f), Eqs. (9)). The domain of attraction of the lower-right stable point is gradually reduced with increasing the value of ε

Thirdly, we numerically compared two methods for the phenomenological modeling of the anergy (inhibition of proliferation) of cytotoxic T-lymphocytes: (a) explicit dependence of the proliferation rate on the current concentration of the virus, and (b) similar dependence of the proliferation rate, but on the accumulated viral load. We showed that under the slow kinetics of the accumulated viral load, this variable should be explicitly considered in the model. This aspect is important for the process of construction of general kinetic models (in biology, chemistry, etc.): model construction should be preceded by the time-scale separation analysis of all variables, and only fast variables can be reduced with Tikhonov's theorem, while the slow variables should be considered as constants or included into the system of equations.

The model considered has many limitations (see the section "Model assumptions"), and weakening, changing or clarifying each of them produces the "degree of freedom" that can be moved along thus giving similar or more complex models. Changes of the model's properties (and rising new ones) during this movements qualitatively compared with experimental data can give information on the general validity of new models. Our work shows that a careful analysis of each, even rather "simple", model demands a lot of work. However, this work should be done.

5. Conclusions

General, low-dimensional models in immunology are not simple ones. They have a variety of behaviors and properties: bistabilities, thresholds, oscillations, etc. Thus, these models can be studied

using approaches and methods of qualitative analysis of differential equations. Clarification of these qualitative models will undoubtevely lead to new discoveries, as we know from the examples from other fields, say blood coagulation, where decades of years and dozens of different models produced a fascinating picture of knowledge of the space- and time-depending processes and mechanisms of their regulation [Tokarev, Ratto, Volpert, 2019].

References

Banerjee M., Tokarev A., Volpert V. Immuno-epidemiological model of two-stage epidemic growth // Math. Model. Nat. Phenom. — 2020. — Vol. 15. — P. 1–11.

Bocharov G. et al. Modelling the dynamics of virus infection and immune response in space and time // Int. J. Parallel, Emergent Distrib. Syst. — 2017. — Vol. 34, No. 4. — P. 341–355.

Bocharov G. et al. Interplay between reaction and diffusion processes in governing the dynamics of virus infections // J. Theor. Biol. — 2018a. — Vol. 457. — P. 221–236.

Bocharov G. et al. Mathematical immunology of virus infections. — Cham, Switzerland: Springer, 2018b. — P. 1–245.

Bocharov G. A. Modelling the dynamics of LCMV infection in mice: Conventional and exhaustive CTL responses // J. Theor. Biol. — 1998. — Vol. 192, No. 3. — P. 283–308.

Dormand J. R., Prince P. J. A family of embedded Runge – Kutta formulae // J. Comput. Appl. Math. — 1980. — Vol. 6, No. 1. — P. 19–26.

Ermentrout B. Simulating, Analyzing, and Animating Dynamical Systems. A Guide to XPPAUT for Researchers and Students. — Philadelphia: Society for Industrial and Applied Mathematics, 2002.

Hunter J. et al. Matplotlib: Visualization with Python.

Marchuk G. I. Mathematical models in immunology. Numerical methods and experiments. — Moscow: Nauka, 1991. — No. 3.

Nicholson L. B. The immune system // Essays Biochem. — 2016. — Vol. 60, No. 3. — P. 275–301.

Romanyukha A. A. Mathematical models in immunology and epidemiology of infectious diseases. — Moscow: Binom, 2012.

Tokarev A., Ratto N., Volpert V. Mathematical modeling of thrombin generation and wave propagation: from simple to complex models and backwards // BIOMAT 2018 International Symposium on Mathematical and Computational Biology. — Springer, 2019. — P. 1–22.